Monte Carlo and molecular-dynamics investigation of [001] twist boundaries in Cu_3Au at $T = 0$ K

A. J. Patrinos
Solid State Science and Technology, Syracuse University, Syracuse, New York

I. P. Antoniades and G. L. Bleris
Physics Department, Aristotle University of Thessaloniki, GR-54006, Thessaloniki, Greece
(Received 15 February 1995; revised manuscript received 9 May 1995)

Sixteen [001] twist boundaries in Cu_3Au spanning a wide range of misorientation angles are investigated at $T = 0$ K using the molecular dynamics and Monte Carlo techniques within the framework of the coincident site lattice approach. Grain boundary (GB) energies vary smoothly with misorientation angle and are described satisfactorily by formulas derived from the theory of dislocations. The equilibrium volume expansion at the GB, and relaxations parallel and normal to the GB plotted against misorientation angle θ all follow Read-Shockley type behaviors. The energies of the unrelaxed GB's are found to be essentially independent of misorientation angle. The structure of low-angle GB's is found to be in agreement with theoretical expectations. Relaxation parallel to the GB works complementarily to relaxation normal to it so as to optimally fix the destroyed stacking at the GB due to twist.

I. INTRODUCTION

Dislocation models have long been known to provide a good description of the structure, energy, and physical properties of low-angle grain boundaries (GB's) in terms of dislocation arrays (edge dislocations for pure tilt GB's or screw dislocations for pure twist GB's). This theoretical approach, however, breaks down for misorientation angles greater than $\sim 15°$ to 20°, above which dislocation cores start to overlap and there ceases to be a meaningful distinction between a dislocation's strain field (which is described by linear elasticity theory) and the core region. Moreover, within the framework of the coincidence site lattice (CSL) approach there have been many arguments concerning the occurrence of cusps in the energy vs angle curves of twist GB's (among others, Refs. 1–3). Whereas in the case of tilt boundaries such cusps have been demonstrated to occur centered around *special* misorientation angles, the situation is not as clear with twist GB's. It seems that the occurrence or not of such cusps is determined to some extent by the potential used in the calculations and that the smoother the potential used, the smaller the cusps observed.[2,4] Based on the limitation to low-angle GB's there are two basic approaches to obtaining a first-principles formula describing the GB energy, γ, as a function of misorientation angle θ: (i) The Read-Shockley (RS) approach[5] and (ii) the Van de Merwe (VM) (Ref. 6) approach. Attempts have also been made to describe cusps within the framework of linear elasticity and secondary dislocations.

The basic relationship obtained by the RS approach is[5]

$$\gamma(\theta) = 2\gamma_0 \sin\frac{\theta}{2}\left[A - \ln\left(2\sin\frac{\theta}{2}\right)\right]. \tag{1}$$

Since for low angles $2\sin\frac{\theta}{2} \approx \theta$, we can write the above as

$$\gamma(\theta) = \gamma_0\theta(A - \ln\theta), \tag{2}$$

where γ_0 is a constant that depends on the elastic constants of the material. For *twist* GB's $\gamma_0 = Kb/2\pi$, where K is the shear modulus. For crystalline systems K is given by elasticity theory of anisotropic media. b is the magnitude of the Burger's vector of the dislocations. Parameter $A = \ln(\frac{e\,b}{2\pi r_0})$ depends on r_0, an effective radius defining the extent of the core of the dislocations. The energy contribution of the *inelastic* strain field inside the dislocation cores is ignored. This approximation is justified in the low-angle limit since the spacing D between consecutive dislocations (given by Frank's formula and discussed below) is large enough compared to r_0. The RS formula is derived based on linear elasticity theory of *continuous* media in the sense that it ignores the discreteness of the lattice in the region of the GB. The RS formula describes GB energies well for misorientation angles $\theta <\sim 5°$, deviating considerably from experimental results at higher angles.

At the same time as Read and Shockley, Van de Merwe derived a similar formula based on the Peierls-Nabarro[7–9] dislocation model. Stresses normal to the boundary are ignored (as they are in the RS approach). The formula for the energy for a *twist* boundary is

$$\gamma(\theta) = \frac{\mu_0 b}{2\pi^2}\left[1 + \beta - \sqrt{1+\beta^2} - \beta\ln(2\beta\sqrt{1+\beta^2} - 2\beta^2)\right], \tag{3}$$

where $\beta = A\tan(\frac{\theta}{2})\sec(\frac{\theta}{2})$ with $A = 2\pi\mu/\mu_0$. Here, μ_0 is the shear modulus of the perfect crystal and μ is an

effective shear modulus of the relaxed structure, which is different from μ_0 due to the presence of dislocations. From parameter A one obtains the effective radius, r_0, of the core of the screw dislocations: $r_0 = bA/4\pi$. Equation (3) describes GB energies better than (1) for angles greater than 5° but fails for angles greater than $\sim$ 15°. An empirical extension of Eq. (2) can be arrived at by replacing θ by $\sin(m\theta)$:

$$\gamma(\theta) = \gamma_0^* \sin m\theta [A^* - \ln(\sin m\theta)], \tag{4}$$

where m is an integer whose value depends on the symmetry of the CSL describing the boundary and determines the maximum of the curve of Eq. (4). m is equal to 2 for [001] GB's in cubic crystals due to the fourfold symmetry of the CSL. γ_0^* and A^* are fitting parameters. This empirical formula was first introduced by Wolf[3,10] in the simulation of symmetrical tilt and twist grain-boundaries in Cu and Au. He found Eq. (4) could fit energy vs angle simulation data in the entire range of misorientation angles and proposed that low angle data could be used to predict grain-boundary energies at high misorientation angles. However, the disadvantage of Eq. (4) is that it is difficult to assign physical significance to the parameters γ_0^* and A^*,[10] in contrast to the corresponding parameters calculated from first principles in the RS and VM formulas.

It is important to mention that both the RS and the VM equations can fit the energy vs angle curve in the entire misorientation angle range almost as well as Eq. (4) provided that one accepts the loss of physical significance of the fitting parameters. We discuss this further in Sec. III.

In this work:

(1) We obtain energy vs misorientation angle simulation data of [001] twist GB's in the Cu_3Au alloy at $T = 0$ K in a broad angle range (6.7°–43.6°) and CSL multiplicities $\Sigma 5$–$\Sigma 145$.

(2) We test the applicability of the RS and VM equations in the angle range $\sim$ 7°–20°.

(3) We discuss the volume expansion at the GB in a direction perpendicular to the GB.

(4) We compare and contrast the relaxed structures obtained for low- and high-angle boundaries as well as the fine structure of the energy vs angle curve.

The simulations were performed using the Monte Carlo (MC) and molecular dynamics (MD) methods on CSL's ranging from $\Sigma 5$ to $\Sigma 145$. In the past MD, lattice statics, and conjugate gradient were almost exclusively the methods of choice for relaxation simulations at 0 K. In contrast, the computationally more expensive MC methods have been favored in situations where MD is impossible or difficult to apply, such as the simulation of order-disorder transitions in alloys and constant temperature situations among others. However, by exploiting the fact that from one MC step to the next there are only local changes to the lattice, one can significantly speed up the MC calculations to a point that they become competitive to MD. With this in mind we have performed a comparative study of $\gamma(\theta)$ using both methods. The use of both methods provides us with (as a by-product) a consistency check of our results.

II. SIMULATION DETAILS

The development of high-performance computers has made possible the use of many-body interaction potentials that have been proven more realistic in simulations of metals and metal alloys than the simpler in calculation but also more simplistic pair potentials. The potential used in this study is a many body potential of the Finnis and Sinclair type[11] and is given by the sum of a repulsive term E_B and an attractive one, E_N:

$$E = E_B + E_N, \tag{5}$$

respectively given by

$$E_B = \sum_{\alpha}^{N_\alpha} \sum_{i=1} \left(\sum_{\beta}^{N_\beta} \sum_{\substack{j=1 \\ j \neq i}} A_{\alpha\beta} e^{-p_{\alpha\beta}\left(\frac{r^{\alpha\beta}}{d^{\alpha\beta}} - 1\right)} \right) \tag{6}$$

and

$$E_N = \sum_{\alpha}^{N_\alpha} \sum_{i=1} \left(\sqrt{\sum_{\beta}^{N_\beta} \sum_{\substack{j=1 \\ j \neq i}} \xi_{\alpha\beta}^2 e^{-2q_{\alpha\beta}\left(\frac{r^{\alpha\beta}}{d^{\alpha\beta}} - 1\right)}} \right). \tag{7}$$

In the above expressions α and β denote the atomic species (in our case Cu and Au), A, p, q, and ξ are the potential parameters of the respective interaction terms, d is the nearest neighbor distance for the respective material, and N, which depends on the cutoff radius, is the number of neighbors considered for each respective atom.

Parameters appropriate to the above potential have been previously determined and published, most recently in Refs. 12–14. These parameters were found to satisfactorily reproduce material parameters such as the lattice constant, cohesive energy, and bulk modulus for the Cu-Au alloy system over the entire range of relative concentrations.

Many body potentials are probably the most realistic for the simulation of covalent metals and alloys. Their main drawback is their complexity and the large number of neighbors that have to be included into the calculation. However, most of the effort to calculate the potential at some (noninitial) step is repetitive and, therefore, superfluous and can be avoided by carefully calculating changes to the potential from one step to the next. There are two cases where such modifications can result in dramatic speed increases in its calculation, both applicable to MC simulations. The principle that applies is the same in both cases, namely a change in the coordinates of one atom or an exchange of the coordinates of two atoms of differing species, and is that for small changes in the lattice it is possible to correct the potential calculated for the original state of the lattice by the amount corresponding to the change in state. The computational effort for such a correction is much less than that required for calculating the potential of the lattice anew.

The 50 to 500-fold speed increase (depending on the size of the lattice) is well worth the extra programing effort and resulting code complexity.

The MD experiments were performed using the classical Hamiltonian given by $H = \sum_i \frac{p_i^2}{2m_i} + E$, where the summation extends over all atoms i in the lattice, m_i and p_i are the conjugate masses and momenta of atom i, and E is the potential as defined in Eq. (5). The equations of motion were integrated using the finite difference scheme of Verlet.[15–17]

Typical periodic boundary conditions were used in all simulations. The sizes of the systems considered ranged from 1200 to 13 920 atoms. In all cases 12 atomic planes were included on either side of the boundary in order to avoid interactions with its image GB formed because of the periodic boundary conditions in the direction [001]. The size of the lattice in the plane of the boundary is determined by the size of the CSL, which can be quite large for large values of Σ. The basis of the lattice is composed of two atoms (Cu, Au). As a result, the size of unit CSL for the alloy is double of that corresponding to a single element. The cuttoff radius for the potential was $R_c = 1.7a$, where $a = 3.748 \times 10^{-8}$ is the average latice parameter of the Au-Cu perfect lattice structure.

Runs were stopped when $\Delta E/E \leq C/N$, where $\Delta E/E$ is the fractional change in the running average of the energy (within the last 10^5 MC steps), C is a "tolerance" which is the same for all runs, and N the number of atoms in a particular computational cell. In MC runs C was set equal to 2×10^{-5} (a quite stringent condition) for all runs resulting in satisfactory equilibration after about 1500–2000 moves per atom. A similar termination criterion was used for the MD experiments.

The simulations were performed using initial structures with atoms at their nominal coordinates. In the case of monatomic metals and nonmetallic systems the existence of a local volume expansion at the GB in a direction normal to the GB has been experimentally verified by microscopic observations[18,19] and computer simulations.[10,20] In this work local volume expansion at the GB was handled by realizing constant volume experiments at a range of *initial* volume expansions, ΔV_0, where ΔV is defined by[4] $d/d_0 - 1$, d_0 being the nominal distance between atomic planes in the crystal in the direction normal to the boundary and d the width of the expanded GB. No account was taken of rigid body translations of the two parts of the bicrystal in a direction parallel to the boundary. This choice is justified in [001] twist GB's by previous simulation results[21,22] in which such relaxations are energetically of far less importance than those perpendicular to it with the exception of $\Sigma 5$ for which previous careful simulation studies have shown that initial configurations produced by relative parallel translation of the two crystallites in the CSL structure by primitive DSC lattice vectors may result in slightly lower relaxed GB energies than when the CSL is used as the initial structure.[23,24]

The minimum energy and the corresponding value of the equilibrium volume expansion, $\Delta V_{\min}$, were determined by least-squares polynomial fits. It is interesting to note that the RS and VM formulas do not consider the volume expansion at the GB because they assume zero stresses normal to the boundary. This assumption is justified for very low-angle GB's since the magnitude of the expansion there is indeed small. At higher angles the assumption breaks down, a fact that constitutes an extra discrepancy factor with respect to experimental data.

III. RESULTS AND DISCUSSION

A. Energy and volume expansion vs twist angle

In the present work, both the MC and MD runs were performed at a range of grain-boundary widths, d, in order to determine the value of ΔV corresponding to the minimum in grain-boundary energy, $\gamma(\Delta V_{\min})$. For each CSL five different values of initial volume expansion ΔV_0 in the range 0.0–0.4 were used. Figure 1 shows the relaxed grain-boundary energies, γ, as a function of ΔV_0 for various CSL's (MC results). Second and in some cases fourth degree polynomial fits were performed to determine $\Delta V_{\min}$. The values of the energy and corresponding volume expansions are shown in Fig. 2 for MC and MD runs. One sees that the energy vs twist angle curves are essentially smooth with no indication of cusps at low Σ CSL's (e.g., $\Sigma 5$ or $\Sigma 13$). The results show a monotonous increase up to approximately 33°, above which the energy levels off. The fit to the Wolf relation is excellent. We observe that $\Delta V_{\min}$ follows the same qualitative behav-

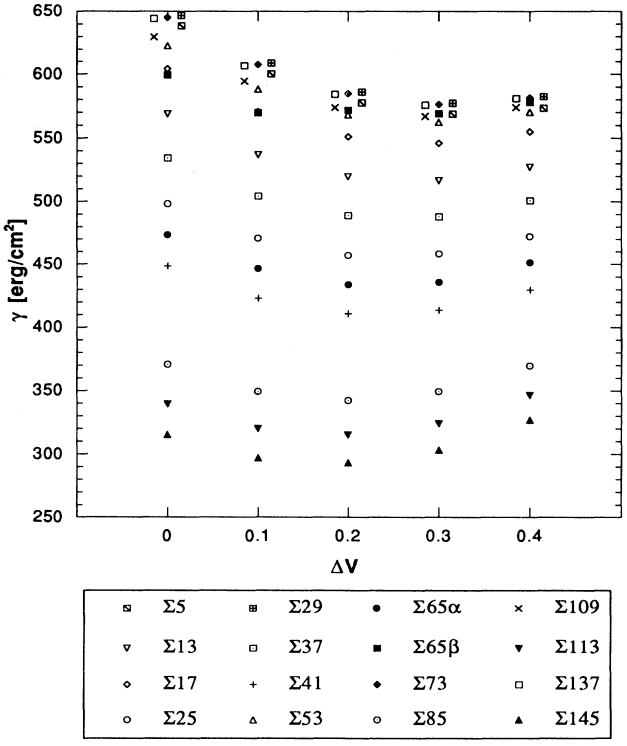

FIG. 1. Dependence of grain-boundary energy γ on ΔV for each Σ. Some data sets at the top of the plot have been horizontally displaced for clarity (MC runs).

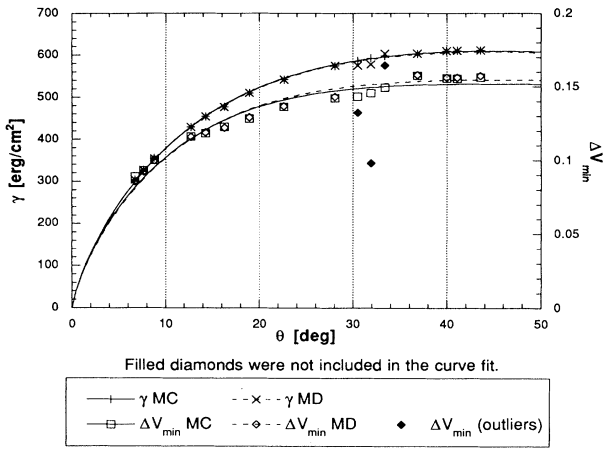

FIG. 2. Grain-boundary energy and volume expansion at the boundary corresponding to minimum energy as a function of misorientation angle (MC and MD runs).

ior with respect to angle as the energies with an anomaly appearing in the MD data at $\Sigma 53, \Sigma 65b$, and $\Sigma 109$. The runs for these systems were repeated at stricter tolerances (almost down to machine precision) but to no avail. Even though there is no significant effect on the respective energies, the discrepancy, if real (as opposed to numerical, such as insufficient equilibration), is puzzling and is related perhaps to the transition into the plateau region of the $\gamma(\theta)$ curve. There is remarkable agreement in the energy obtained by the two methods with both sets of results following an RS-like behavior. The small discrepancies that appear at $\Sigma 53$, $\Sigma 65b$, and $\Sigma 109$ are presumably related to the respective discrepancies in the volume expansions. The parameters of the above fits are summarized in Table I. Errors from the fits were insignificant.

Equation (2), as already mentioned, provides a good description of the energies $\gamma(\theta)$ for angles less than about 5°. Such low angle boundaries are described by CSL's of

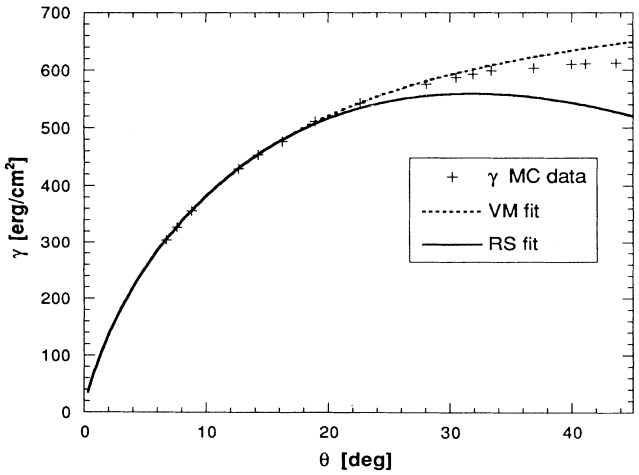

FIG. 3. Fits to RS [Eq. (1)] and VM [Eq. (3)] expressions. Data points with $\theta < 20°$ were used for the fits (MC runs).

TABLE I. Parameters extracted from fits to grain-boundary energy vs misorientation angle data.

	γ_0	A	A_{VM}	b	r_0
Low-angle RS	2345.8	0.17		0.855	0.31
Low-angle VM	2367.2		6.12	0.863	0.42
Wolf	463.6	1.31		-	-

large multiplicities ($\Sigma > 145$) which are difficult to simulate. However, Eq. (2) can be fitted to energy data quite well for higher angles with fit parameters that lose their physical significance in terms of the shear modulus, K, and magnitude, b, of the Burger's vector. Because the boundaries in the present work are all above 5° in angle, we attempted, following the method by Doni and Bleris,[25] a linear least-squares fit of $\gamma(\theta)/[2\sin(\theta/2)]$ vs $\ln[2\sin(\theta/2)]$ (using the MC results) in the angle range 5°–20° in order to determine the deviation of the fit parameters from the expected theoretical values of the RS formula. The resulting curve is shown in Fig. 3 extrapolated over the entire misorientation range. As seen in Table I, from the fit parameters we extracted a value for $b = 0.855a$, where a the average lattice parameter. For this calculation we used an effective value of the shear modulus K which we calculated[26] from the values of the anisotropic elastic constants of the Cu_3Au system reported for 0 K in Ref. 13. The expected value of b is $0.707a$ (the magnitude of $\mathbf{b} = \frac{1}{2}[110]$, the Burger's vector of the screw dislocations characteristic of fcc structures[26]). A fit to the VM formula for angles less than 20° was also performed. The result is shown in Fig. 3 whereas the fit parameters are included in Table I. We notice that there is almost exact agreement between the RS and VM fit parameter γ_0 in the low angle range. The values of r_0, however, slightly disagree because the radii of the cores of the screw dislocations are obtained by different approaches in the two theories. The value obtained by the VM fit is larger than the value obtained by the RS fit. (See the discussion in Sec. III D.)

As in Ref. 25, we attempted a comparison of the RS and VM curves for the parameter values obtained from the fits to low-angle data with the energy data in the entire angle range. The comparison is shown in Fig. 3. For the RS curve we used the exact RS relationship [Eq. (1)], since we plot the formula in the entire angle range. We observe that both fits (RS and VM) are almost identical at angles less than 20°. At larger angles the RS curve has, as expected, an early maximum whereas the maximum of the VM curve occurs at an angle greater than 45°. In addition, the VM curve approximates energy data better than the RS curve at larger angles, as it was also expected. The VM formula, using the fit parameters which are approximately 20% different from the experimental ones, gives a satisfactory approximation to the data for angles up to about 33°. The values we obtained for r_0 are reasonable for metals.[26]

At finite temperatures vibrational and configurational entropy terms must be included in the expression of GB

free energy. The change in relative atomic species concentration in the bicrystal as well as segregation effects at the GB region become important. A recent study[27] of [001] twist GB's in a Cu-Ni system at finite temperatures showed that the GB free energy drops with increasing temperature indicating that the GB possesses a positive excess entropy. The GB free energy vs misorientation angle curves all showed RS-type behavior for all the temperatures studied. Small inflections were observed in the vicinity of the $\Sigma 5$ boundary. Other extensive studies showing the effect of temperature on segregation and [001] twist GB structure of binary metal alloys were presented in Refs. 28–33. We must note that in this study we did not consider the effects of varying the chemical potential at the boundary as a first approximation to twist GB's in the Cu_3Au system. Varying the relative concentrations at the GB of the two metal species in a binary alloy can further reduce the GB energy even at T=0 K.[33] However, in light of previous studies on other alloys, we expect no qualitative changes to the form of the GB energy vs misorientation angle curves of [001] twist GB's in our system.

B. Volume expansion normal to the grain boundary

Although there is no general quantitative theory that describes the magnitude of $\Delta V_{\min}$, such an expansion is expected. When two perfect crystallites are misoriented by twist with respect to each other and are placed at a distance equal to their distance in the perfect lattice, the destruction of perfect stacking at the GB causes the interatomic distances of the atoms lying closer to the GB and on either side of it to be increased for some atoms and decreased for others (compared to their respective distances in the perfect crystal). However, the repulsive part of the interaction potential varies much faster with distance than the attractive part, resulting in an overall tendency of the misoriented crystals to repel. This happens for initial values of volume expansion (imposed in the simulation) $\Delta V_0 < \Delta V_{\min}$. For $\Delta V_0 > \Delta V_{\min}$ the situation is reversed as a result of the shorter range of the repulsive forces as compared to that of the attractive ones. (See also Ref. 34.)

Figure 4 shows the equilibrium energies of the GB as a function of $\Delta V_{\min}$ (MC results). The almost linear dependence of γ on $\Delta V_{\min}$ agrees with theoretical, computational, and experimental results on monatomic metals.[35] We notice, however, that there is a deviation from linearity at the last six or so data points corresponding to the highest angle GB's ($\theta > 30°$). The curve reaches a plateau indicating a sort of "saturation" of GB energy with respect to volume expansion above a certain value, a fact that has not been observed in the results of other authors. The error bars represent our estimates of standard error in the values of $\Delta V_{\min}$ which comes from the uncertainty in the polynomial fits of energy vs ΔV data already mentioned. Despite the uncertainties in the $\Delta V_{\min}$ values, the trend towards a plateau is clear.

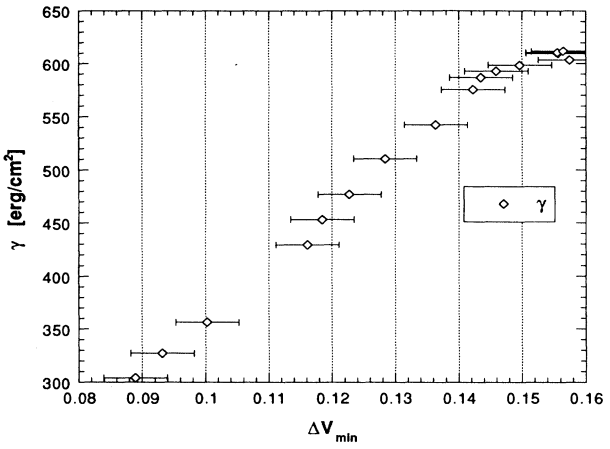

FIG. 4. Equilibrium GB energies vs volume expansion $\Delta V_{\min}$.

C. Grain-boundary energies of unrelaxed CSL structures

Unrelaxed CSL energies were found to be essentially independent of misorientaion angle (or multiplicity Σ) except for a 40 erg/cm^2 cusp at $\Sigma 5$ and $\Delta V = 0$, which, however disappeared at the other volume expansions. Qualitatively, this fact is justified as follows: in twist GB's interatomic distances in the GB region are altered only due to the relative displacement of the two crystallites in a direction *parallel* to the GB; there is no change in the interplanar distances between parallel to the GB planes. On the contrary, the introduction of a tilt misorientation alters interplanar distances of parallel to the tilt GB planes by an amount which depends on Σ. As a consequence, deep cusps occur in both unrelaxed and relaxed energy vs tilt angle curve at some values of Σ for which the change in interplanar distance is much smaller than CSL's of nearby tilt angles but with different value of Σ^2. The parallel displacements due to twist, however, cause change of interatomic distances that are on the overall almost of the same magnitude for GB's of any twist angle, provided that the bicrystal is a multiple of CSL units. Thus the GB energies of the unrelaxed CSL structures themselves are expected to be very similar for all GB's of different misorientation angles. Deviations from this pattern should occur only for very low Σ boundaries ($\Sigma 5$ for example) due to the relatively higher percentage of atoms which lie on perfect lattice positions. These deviations should cause only small dips in the unrelaxed energy vs misorientation angle curves, because they involve only a small fraction of atoms.

D. Relaxed structures

The following discussion in this section and the next refers to both the MD and MC experiments since both methods yielded essentially indistinguishable results. The structure of low angle twist boundaries is

known to be described by a grid made up of two sets of *screw* dislocations. For symmetrical twist boundaries, such as the [001] boundaries examined here, the two sets of dislocations are perpendicular to each other. Consecutive dislocations in the one set are separated by a distance D given by Frank's formula:

$$D = \frac{b}{2 \sin \frac{\theta}{2}}, \tag{8}$$

where b is the magnitude of the Burger's vector and θ the misorientation angle. Figure 5 shows the structure of four (002) planes (two on either side of the GB) for $\Sigma 145$, a low angle boundary ($\theta = 6.7°$). The [001] direction points out of the paper. There are apparent regions of perfect lattice structure surrounded by two sets of screw dislocations. The sense ξ_1, ξ_2 of each set is parallel to its respective Burger's vector $\mathbf{b_1} = \frac{1}{2}[110]$ and $\mathbf{b_2} = \frac{1}{2}[\bar{1}10]$, as seen in the figure. Some lines of the strain field that show the deformation of crystal structure inside the cores of the dislocations are also drawn. The continuous line corresponds to the lower two planes whereas the dashed one to the upper ones. Concentrating on the dislocation arrays that surround a single perfect crystal region, we observe that the strain field inside the core of the same dislocation, same distance from the boundary but on opposite sides, is different. This is because the boundary is centered between a mixed Cu-Au and a pure Cu (001) plane. The binary nature of our system is the cause of the twofold (instead of fourfold) symmetry of the dislocation arrays lying in the same (001) plane.

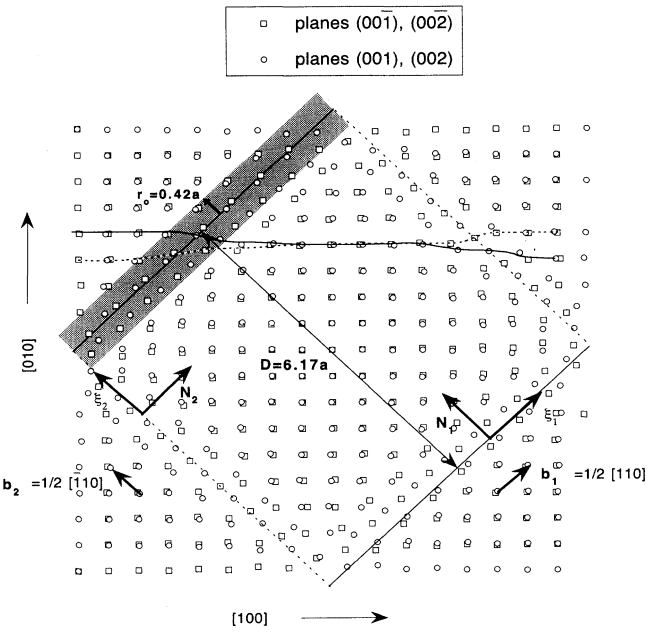

FIG. 5. (001) projection of relaxed structure of $\Sigma 145$ (z-axis points out of the paper). The square frame made up of continuous and dashed lines marks two members for each set of dislocations making up the twist boundary, same type of line indicating same set of dislocations. The curved bold and dashed lines are eye-guiding curves that follow roughly the strain field of two parallel to the boundary atomic rows: a row at positive z values (continuous line) and a row at negative z values (dashed line). The core of the dislocations, as obtained from the VM fit, is marked inside the shaded region.

We have also marked the extent of the dislocation core $r_0 = 0.42a$ obtained from the VM fit in Sec. III A. Looking at the figure at grazing angle we notice that this value appears reasonable compared to the actual relaxed structure obtained from the simulation. From Fig. 5 we measured the distance between consecutive dislocations and found it equal to $D = 6.17 \pm 0.22a$. Inserting this value into Eq. (8) gives a value for the magnitude of the Burger's vector $b = 0.72 \pm 0.025a$, which agrees within standard error with the expected value of $0.707a$.

E. Structural effects

In order to look at some structural aspects of the relaxation process in the entire misorientation angle range we additionally measured the average difference per atom of the atomic positions in the relaxed structure from their respective positions in the unrelaxed CSL structure:

$$\langle \Delta R_{xy} \rangle \equiv \frac{1}{M} \sum_{i=1}^{M} \left[\left(x_i^{\mathrm{CSL}} - x_i^{\mathrm{rel}} \right)^2 + \left(y_i^{\mathrm{CSL}} - y_i^{\mathrm{rel}} \right)^2 \right]^{1/2}, \tag{9a}$$

$$\langle \Delta R_z \rangle \equiv \frac{1}{M} \sum_{i=1}^{M} \left(z_i^{\mathrm{CSL}} - z_i^{\mathrm{rel}} \right), \tag{9b}$$

where M is the number of atoms over which we wish to average, $(x_i^{\mathrm{CSL}}, y_i^{\mathrm{CSL}}, z_i^{\mathrm{CSL}})$ is the position vector of atom i in the unrelaxed CSL structure and $(x_i^{\mathrm{rel}}, y_i^{\mathrm{rel}}, z_i^{\mathrm{rel}})$ is the respective position in the relaxed structure. Axis z is normal to the boundary. We will refer to the quantities inside $\langle \cdots \rangle$ in Eq. (9) as *average relaxation length* parallel and perpendicular to the GB, respectively. For the calculations of the quantities in Eq. (9) we used MD data for *zero* initial volume expansions. Figure 6 shows the dependence of the average relaxation length *parallel* to the GB, $\langle \Delta R_{xy} \rangle$, on misorientation angle, where the average is taken over all atoms in the computational cell (left y axis). We observe that the relaxation length is reduced as the angle increases in an RS fashion after reversing the sense of the ordinate. Figure 6 also shows the respective average relaxation, $\langle \Delta R_z \rangle$, in a direction normal to the GB (right y axis). The average is taken over all atoms in the first six planes on the positive z axis (i.e., planes 001 to 006) which are the planes affected by the *real* GB at $z = 0$ and not by its image at the edge of the computational cell. All $\langle \Delta R_z \rangle$ values are negative. According to Eq. (9b), this can be interpreted as an overall tendency of atoms on one side of the GB to relax away from it, as already discussed in the Sec. III B. The shape of the curve is again of RS type. As the angle increases, the *absolute value* of the average relaxation length increases, as expected. Comparing $\langle \Delta R_{xy} \rangle$ to $\langle \Delta R_z \rangle$ values in Fig. 6 we conclude that the greater the average relaxation par-

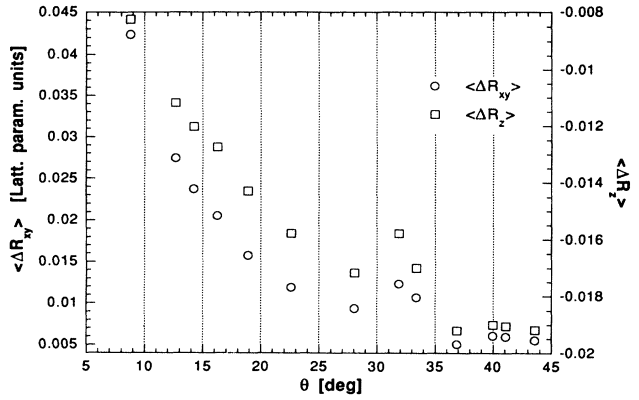

FIG. 6. Average relaxation length per atom in directions parallel and normal to the GB as a function of misorientation angle.

allel to the GB, the smaller the average relaxation in a direction normal to it (notice the complementary character of the small cusp at $\Sigma 5$). The previous remark is demonstrated explicitly in Fig. 7 which shows a log-linear plot of the average relaxation length parallel to the GB vs the absolute value of the average relaxation length normal to the GB. Except for the last four points, shown in a circle, corresponding to the four largest angle boundaries ($\Sigma 5, \Sigma 137, \Sigma 73, \Sigma 29$), the others follow an almost exponential decrease, as indicated by the dashed straight line used as a guide to the eye. This decrease of the relaxation perpendicular to the GB with increasing relaxation parallel to it can qualitatively be understood in conjunction with the discussion on the volume expansion at the GB in Sec. III B: the atomic relaxation occurs in such a fashion as to restore the perfect stacking of atoms at the GB which was destroyed by the introduction of twist. This can be done in two modes: (i) *parallel relaxation*, i.e., by twisting back parts of the crystal at the GB, thus restoring the broken bonds; (ii) *normal relaxation*, i.e., the volume expansion at the GB that we already discussed, which restores interatomic distances that were reduced by the introduction of twist, bringing them closer to their perfect lattice values. These two modes are complementary to each other meaning that when one mode is stronger the other is suppressed. In low angle boundaries for large parts of the boundary linear elasticity holds and there is a restoring torque opposing the small perturbation of twist. Thus relaxation occurs according to mode (i) and mode (ii) is suppressed. On the contrary, in large angle boundaries there is little or no net restoring torque. Thus relaxation occurs mostly by mode (ii).

We also compared and contrasted the relaxation of Cu atoms to that of Au atoms. First, in a direction parallel to the GB [see Fig. 8(a)] the average relaxation length

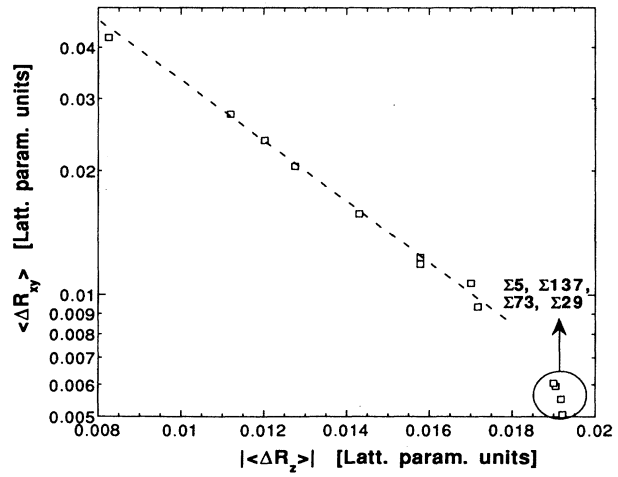

FIG. 7. Average relaxation length in a direction parallel to the GB vs the absolute value of average relaxation length normal to the GB.

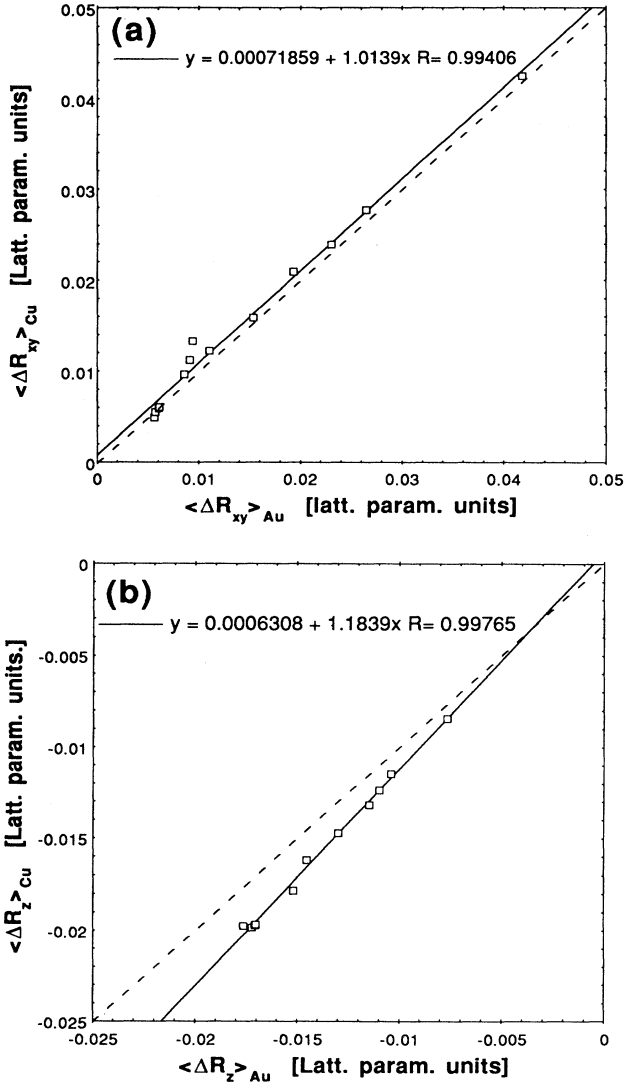

FIG. 8. Average relaxation length of Cu atoms vs average relaxation length of Au atoms: (a) parallel to the GB (b) normal to the GB. The dashed line is the $x = y$ line.

parallel to the GB of Cu atoms varies linearly with the respective average relaxation length of Au atoms and actually $\langle \Delta R_{xy} \rangle_{\mathrm{Cu}} \approx \langle \Delta R_{xy} \rangle_{\mathrm{Au}}$ for all angles θ as depicted by the linear least-squares fit in Fig. 8. On the contrary, in a direction normal to the GB, comparison of relaxation lengths between the two atomic species in a direction normal to the GB shows that Cu atoms relaxed more than Au atoms with respect to their unrelaxed CSL positions [see Fig. 8(b)]. Finally, we examined the average relaxation lengths per xy plane vs distance z from the GB for each of the atomic species, Au and Cu [Figs. 9(a)–(d)]. The averages $\langle \cdots \rangle$ in Eqs. (9) are taken over atoms in each xy plane. In Figs. 9(a), and 9(b) we plot relaxation lengths parallel ($\langle \Delta R_{xy} \rangle$) and normal ($\langle \Delta R_z \rangle$) to the GB for $\Sigma 29$, a high angle boundary ($\theta = 43.6°$), whereas in Figs. 9(c) and 9(d) the respective relaxation lengths for $\Sigma 85$, a low angle boundary ($\theta = 8.8°$). Relaxation length values for Au atoms exist only for mixed planes. The real GB exists at $|z| = 0$ while the image GB at $|z| = 6$. The first plane on the positive z's is a mixed Au-Cu plane whereas the first plane on the negative z's is pure Cu. Pure and mixed planes alternate thereon. The effect of this asymmetry (related to stoichiometry) on relaxation length is evident in Fig. 9.

(1) *Direction parallel to GB*: from Fig. 9(c) we see that for $\Sigma 85$, Cu atoms moved almost exactly the same as Au atoms in every mixed plane. In contrast, for $\Sigma 29$ [Fig. 9(a)], Au atoms moved more than Cu atoms in every plane, the difference becoming more pronounced as we move closer to the GB. Notice that $\langle \Delta R_{xy} \rangle$ varies smoothly with z for the low-angle boundary in contrast to the irregular variation for the large angle one. Also, for $\Sigma 29$, relaxation length of Cu atoms in mixed planes is less than relaxation length of Cu atoms in pure planes.

(2) *Direction normal to the GB*: from Figs. 9(b) and 9(d) we see that for both $\Sigma 29$ and $\Sigma 85$ Cu and Au atoms moved the same amount at all planes except for the first two mixed planes on either side of the GB, where Au atoms moved less. The fact that $\langle \Delta R_z \rangle$ is positive at negative z values and reverses sign at positive z values is easily identified, in conjunction with Eq. (9b) as the expected volume expansion at the GB. Notice also that relaxation length normal to the GB varies linearly with distance from it for all planes with the exception of the two closest to the GB. In addition, $\langle \Delta R_z \rangle$ varies smoothly with z for both low- and high-angle boundaries, in contrast to the variation of $\langle \Delta R_{xy} \rangle$ mentioned before, a fact that indicates a smoother z variation of the stress component normal to the GB than the parallel stress component.

Finally, in all the aforementioned figures, we see that there is absolute symmetry in relaxation lengths between the real and the *image* boundary, whereas there is no symmetry in relaxation lengths between the two sides of the same boundary due to the stoichiometrical asymmetry already mentioned.

IV. CONCLUSIONS

Concluding our discussion we note that both computational methods yielded essentially the same results if one neglects the small discrepancies that occurred between 30° and 35° presumably caused by insufficient equilibration at some MD runs. Moreover,

(1) Energies of [001] twist GB's in a Cu_3Au system at $T = 0$ K vary smoothly with misorientation angle with no indication of cusps at GB's corresponding to CSL's of small multiplicity.

(2) Formulas that are derived from dislocation theory satisfactorily describe the energies of GB's in our system. The equilibrium volume expansion, $\Delta V_{\min}$, at the GB, the average relaxation length parallel, $\langle \Delta R_{xy} \rangle$, and normal, $\langle \Delta R_z \rangle$, to the GB plotted against misorientation

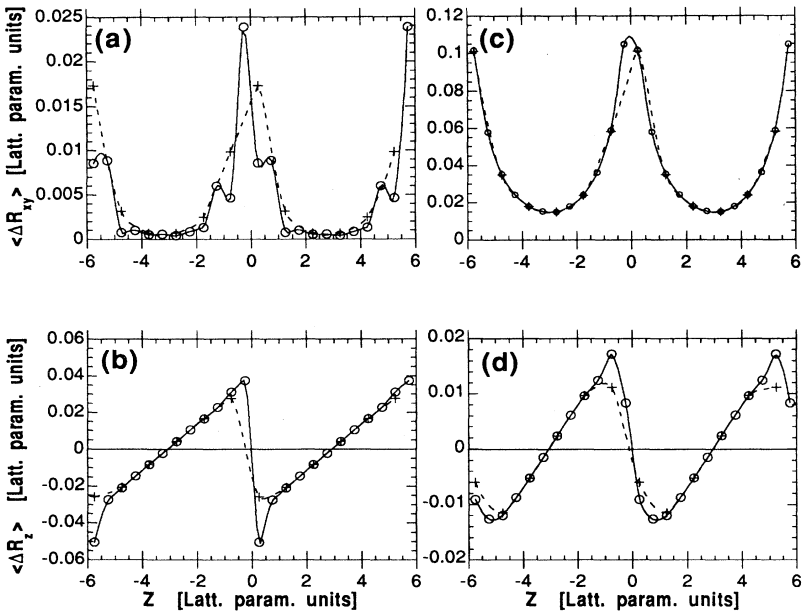

FIG. 9. Average relaxation length per xy plane vs distance z from the GB. (a), (b) Relaxation lengths for $\Sigma 29$ parallel and normal to the GB, respectively. (c), (d) The same as in (a), (b) for $\Sigma 85$. Open circles represent averages over Cu atoms whereas crosses averages over Au atoms. Interpolation curves are included as guides to the eye.

angle all follow RS type behavior.

(3) The energies of the *unrelaxed* CSL structures at all initial volume expansions are independent of misorientation angle (except for a small dip at $\Sigma 5$ for $\Delta V = 0$).

(4) The structure of low-angle GB's in our system is described by a dislocation grid made up of two sets of dislocations perpendicular to each other with Burger's vectors $\frac{1}{2}[110]$ and $\frac{1}{2}[\bar{1}10]$. The distance D between consecutive dislocations of the same set agrees with Frank's formula. The strain field at the same dislocation, same distance from the GB but different side is different due to the binary nature of our system. For the same reason, the strain field at the same plane but different set of dislocations is also different.

(5) Relaxation parallel to the GB works complementarily to relaxation normal to it so as to optimally fix the destroyed stacking at the GB due to twist. Moreover, the average relaxation length parallel to the GB decreases almost exponentially with average relaxation length normal to the GB for angles $\lesssim 37°$. For four GB's with $\theta \gtrsim 37°$ the decrease is much steeper. In fact, we more generally conclude that the behavior of the highest angle boundaries deviates from that of the others as seen in the relaxed GB energy vs twist angle, relaxed GB energy vs volume expansion at equilibrium and parallel relaxation vs normal to the GB relaxation curves.

(6) Average relaxation length parallel to the GB for Cu atoms is approximately the same with that for Au atoms whereas average relaxation normal to the GB is larger for Cu atoms than Au atoms. In addition, for high-angle boundaries, relaxation length parallel to the GB of Cu atoms in mixed planes is less than relaxation length of Cu atoms in pure planes.

ACKNOWLEDGMENTS

We wish to acknowledge the generous financial support of the General Secretariat of Research and Technology of Greece under Project No. ΠΕΝΕΔ 91EΔ334. A. J. P. wishes to thank the Solid State Division of the Physics Department of the Aristotle University of Thessaloniki for its kind hospitality during the course of this work.

[1] A. Brokman and R. W. Balluffi, Acta Metall. **29**, 1703 (1981).
[2] D. Wolf, J. Phys. (Paris) Colloq. **46**, Suppl. 4, C4-197 (1985).
[3] D. Wolf, J. Appl. Phys. **69**, 185 (1991).
[4] D. Wolf, Physica B **131**, 53 (1985).
[5] W. T. Read and W. Shockley, Phys. Rev. **78**, 275 (1950).
[6] J. H. Van de Merwe, Proc. Phys. Soc. London Sect. A **63**, 616 (1949).
[7] R. E. Peierls, Proc. Phys. Soc. **52**, 23 (1940).
[8] F. R. N. Nabarro, Proc. Phys. Soc. **59**, 256 (1947).
[9] J. D. Eshelby, Philos. Mag. **40**, 903 (1949).
[10] D. Wolf, Scr. Metall. **23**, 1713 (1989).
[11] M. W. Finnis and J. E. Sinclair, Philos. Mag. A **50**, 45 (1984).
[12] H. M. Polatoglou and G. L. Bleris, Interface Sci. **2**, 31 (1994).
[13] H. M. Polatoglou and G. L. Bleris, Solid State Commun. **90**, 425 (1994).
[14] M. Polatoglou, K. Magoutis, and G. L. Bleris, Mater. Sci. Forum **126-128**, 623 (1993).
[15] L. Verlet, Phys. Rev. **159**, 98 (1967).
[16] L. Verlet, Phys. Rev. **165**, 201 (1968).
[17] M. P. Allen and D. J. Tildesley, *Computer Simulation of Liquids* (Oxford University Press, New York, 1987).
[18] G. J. Wood *et al.*, Philos. Mag. A **50**, 375 (1984).
[19] K. L. Merkle and D. J. Smith, Phys. Rev. Lett. **59**, 2887 (1987).
[20] K. L. Merkle and D. Wolf, MRS Bull. **XV**, 42 (1990).
[21] P. D. Bristowe and A. G. Crocker, Philos. Mag. A **38**, 487 (1978).
[22] D. Wolf, Acta Metall. **32**, 245 (1984).
[23] V. Vitek, Scr. Metall. **21**, 711 (1987).
[24] D. Schwartz, P. D. Bristowe, and V. Vitek, Acta Metall. **36**, 675 (1988).
[25] E. G. Doni and G. L. Bleris, J. Phys. (Paris) Colloq. **51**, C1-115 (1990).
[26] J. Hirth and J. Lothe, *Theory of Dislocations* (McGraw-Hill Book Co., New York, 1968).
[27] H. Y. Wang *et al.*, Acta Metall. **41**, 2533 (1993).
[28] D. Udler and D. N. Seidman, Phys. Status Solidi B **152**, 267 (1992).
[29] A. Seki, D. N. Seidman, Y. Oh, and S. M. Foiles, Acta Metall. **39**, 3179 (1991).
[30] A. Seki, D. N. Seidman, Y. Oh, and S. M. Foiles, Acta Metall. **39**, 3167 (1991).
[31] I. Majid, C. A. Countermann, P. D. Bristowe, and R. W. Balluffi, Acta Metall. **42**, 3331 (1994).
[32] R. Najafabadi, H. Y. Wang, D. J. Srolovitz, and R. LeSar, Acta Metall. **39**, 3071 (1991).
[33] S. R. Phillpot and J. M. Rickman, J. Chem. Phys. **97**, 2651 (1992).
[34] D. Wolf, Acta Metall. **37**, 2823 (1989).
[35] D. Wolf, Scr. Metall. **23**, 1913 (1989).